Molecular Crystals and Liquid Crystals Science and Technology. Section A. Molecular Crystals and Liquid Crystals
Publication details, including instructions for authors and subscription information:
http://www.tandfonline.com/loi/gmcl19

Theoretical Approaches to Molecular Magnetisms: Through-Bond Couplings Between Triplet Carbenes and Related Species

M. Okumura [a], K. Takada [a], J. Maki [a], T. Noro [a], W. Mori [b] & K. Yamaguchi [a]

[a] Department of Chemistry, Faculty of Science, Hokkaido University, Sapporo, 060, Japan

[b] Department of Chemistry, Faculty of Science, Osaka University, Toyonaka, Osaka, 560, Japan

Version of record first published: 05 Dec 2006.

To cite this article: M. Okumura , K. Takada , J. Maki , T. Noro , W. Mori & K. Yamaguchi (1993): Theoretical Approaches to Molecular Magnetisms: Through-Bond Couplings Between Triplet Carbenes and Related Species, Molecular Crystals and Liquid Crystals Science and Technology. Section A. Molecular Crystals and Liquid Crystals, 233:1, 41-60

To link to this article: http://dx.doi.org/10.1080/10587259308054946

Mol. Cryst. Liq. Cryst. 1993, Vol. 233, pp. 41–60
Reprints available directly from the publisher
Photocopying permitted by license only

Printed in the United States of America

THEORETICAL APPROACHES TO MOLECULAR MAGNETISMS: THROUGH-BOND COUPLINGS BETWEEN TRIPLET CARBENES AND RELATED SPECIES

M. OKUMURA,[a)] K. TAKADA,[a)] J. MAKI,[a)], T. NORO,[a)] W. MORI[b)] AND K. YAMAGUCHI[a,b)]

a) Department of Chemistry, Faculty of Science, Hokkaido University, Sapporo 060, Japan,

b) Department of Chemistry, Faculty of Science, Osaka University, Toyonaka, Osaka 560, Japan

Abstract Ab initio post Hartree-Fock calculations were carried out for polyradical species formed by the through-bond couplings between organic radical groups such as triplet carbenes. Detailed numerical results indicate that the dynamic spin polarization (SP) rules proposed previously are applicable to qualitative predictions of the ground spin states of these species. On the other hand, the spin delocalization (SD) mechanism is operative in the case of polyradicals linked with hetero atoms such as oxygen and nitrogen atoms. The ionized states of polycarbenes and polyenes are also investigated in relation to possibilities of organic magnetic conductors. Computational results are compatible with experimental results available.

INTRODUCTION

Theoretical calculations of effective exchange interactions between radical groups provide a useful guide for molecular design of high-spin molecules. Previously unrestricted Hartree-Fock (UHF) molecular orbital (MO) calculations[1] have been carried out for elucidation of energy gaps between the highest-spin (HS) and lowest -spin (LS) states of poly-carbenes.[2,3] Computational results have indicated that the spin polarization (SP) rule is applicable to qualitative explanations of the ground spin states of neutral polycarbene

systems.[1-3] On the other hand, the spin delocalization (SD) mechanism is found to be operative in the case of polyradicals linked with hetro atoms.[1] The ionized states of polyradical and polyene species have been also investigated in relation to possibilities of organic magnetic conductors.[2,4] However, the refinements of the numerical data by taking into account electron correlation effects have not been performed yet for polycarbenes, although the UHF Møller-Plesset type calculations have been carried out for clusters of free radicals[5] and triplet carbenes[2,6]; namely through-space interaction systems. The basis set dependency of the effective exchange integrals for these clusters have been examined at the UMPn (n=1-4) and approximately spin projected UMPn (APUMPn) levels of the post Hartree-Fock theory.[2] Very recently, the post Hartree-Fock computations[6] such as UNO-CAS, MR CI, UHF QCISD(T), etc. were also carried out for the refiments of the energy gaps between the HS and LS states of polycarbenes and related species, and for confirmation of the previously proposed SP and SD spin alignment rules for the through-bond couplings between radical groups.[1-5] Here , we summarize important aspects revealed by these refinements in relation to previous theoretical work and experimental results available.

SPIN POLARIZATION (SP) AND SPIN DELOCALIZATION (SD) MECHANISMS

Spin Alignment Rules

We have carried out the spin-projected unrestricted Hartree-Fock (UHF) calculations of diradicals and polyradicals in the past decades.[1-5] These computations have revealed that there are two different groups for through-bond spin coupling units: one is ferromagnetic and the other is antiferromagnetic as shown in Fig. 1A and 1B, respectively. The high-spin or low-spin molecules are formed by the through-bond couplings of intrinsic spin in SOMO (NBMO), induced spin by the spin polarization (SP) mechanism, induced spin by the spin delocalization mechanism, etc. The magnitudes of the intramolecular effective exchange couplings (Jab) between these spins are classified into three cases as summarized in Table1. Our computational results[1-5] for these three cases are generally explained by the spin alignment rules based on the SP and SD mechanisms[2] as summarized in Table 2. Figure 2 illustrates schematically typical types of through-bond exchange couplings between spins. However, some violations[7] for the SP and SD rules might occur because of the weak interaction in the case III of Table 1. Probably the refinements such as full geometry optimizations and electron correlation corrections are necessary for such subtle cases. Here these rules are examined by the post Hartree-Fock computations of typical examples.

The High Spin and Low-Spin Energy Gaps

The total energy difference between the lowest-spin (LS) and highest-spin (HS) states in

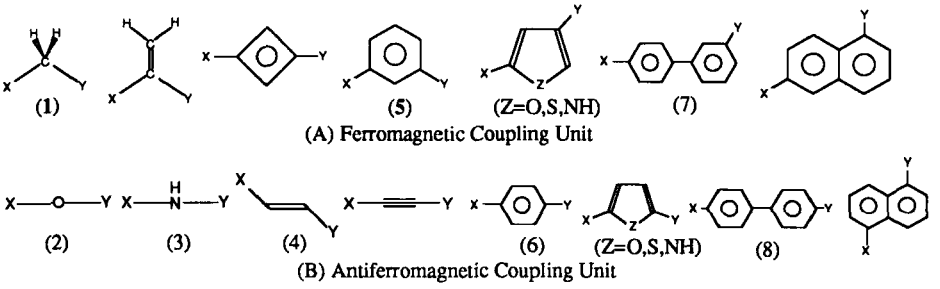

FIGURE 1 Ferro- and antiferromagnetic through-bond coupling units

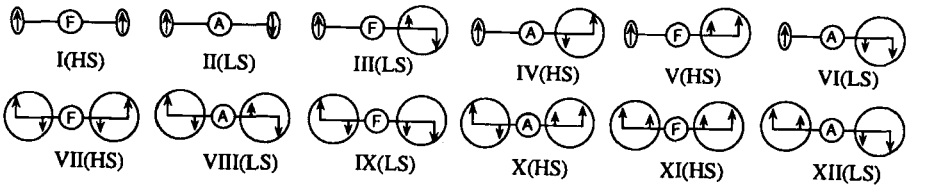

FIGURE 2 Schematic illustrations of intramolecular spin alignments rules. Types I-XII are given in Table 2. F and A denote the ferromagnetic and antiferromagnetic, respectively.

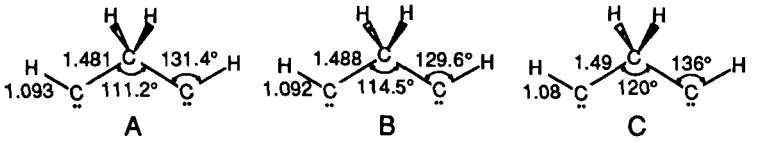

FIGURE 3 The optimized geometries of the quintet (A) and singlet (B) states of bismethylene methane (1a) by the UMP2 6-31G* method and assumed structure (C).

TABLE 1 The through-bond exchange couplings (Jab) between spins (X,Y)[a)]

case	X	Y	|Jab|
I	intrinsic spin in SOMO(or NBMO)	intrisic spin in SOMO(or NBMO)	large
II	intrinsic spin in SOMO(or NBMO)	induced spin by SP(or SD)	medium
III	induced spin by SP(or SD)	induced spin by SP(or SD)	small

a) notations : SP(spin polarization), SD(spin delocalization).

TABLE 2 Intramolecular spin alignment rules[a)]

Type	X	C.U.	Y	G.S.
I	SOMO(NBMO)	F	SOMO(NBMO)	HS
II	SOMO(NBMO)	A	SOMO(NBMO)	LS
III	SOMO(NBMO)	F	negative IS by SP	LS
IV	SOMO(NBMO)	A	negative IS by SP	HS
V	SOMO(NBMO)	F	positive IS by SD or SP	HS
VI	SOMO(NBMO)	A	positive IS by SD or SP	LS
VII	negative IS by SP	F	negative IS by SP	HS
VIII	negative IS by SP	A	negative IS by SP	LS
IX	negative IS by SP	F	positive IS by SD or SP	LS
X	negative IS by SP	A	positive IS by SD or SP	HS
XI	positive IS by SD or SP	F	positive IS by SD or SP	HS
XII	positive IS by SD or SP	A	negative IS by SD	LS

a) notations : C.U. : coupling unit, F : ferromagnetic coupling unit, A: antiferromagnetic coupling unit; IS: induced spin, SP : spin polarization, SD: spin delocalization, HS: high spin, LS: low spin, G.S.: ground spin state.

molecules and oligomers is defined by

$$\Delta E(\text{LS-HS}) = {}^{LS}E_{total}(X) - {}^{HS}E_{total}(X) \quad (1)$$

where ${}^{Y}E_{total}(X)$ denotes the total energy obtained for the spin state (Y) by the post Hartree-Fock methods (X), which are briefly explained in the appendix. As discusssed previously, [8] the spin projection is usually necessary for the LS wavefunctions obtained by the unrestricted Hartree-Fock (UHF) based methods such as UMP, UHF QCISD(T), etc. To this end, our approximate spin projection (AP) procedure[8] is used here, together with Schlegel[9] and Handy[10] spin projection methods as discussed in the appendix.

Spin Polarization (SP) Mechanism

The post Hartree-Fock (HF) calculations by the use of the 6-31G* basis set have been carried out for bismethylene methane **1a** ($CH\text{-}CH_2\text{-}CH$) which is formally formed by the through-bond coupling of two triplet methylenes via the methylene bridge: namely X=Y= -CH in the case of **1** in Fig. 1. Full geometry optimizations of the LS (S=0) and HS (S=2) states of the C_{2v} geometry of **1a** have been performed, respectively, by using the energy gradients of the LS and HS UMP2 wavefunctions. Figure 3 shows the fully optimized geometries A and B in the HS and LS states respectively, together with the assumed geometry C of **1a**. The total energy calculations of the LS and HS states of **1a** at each optimized (A, B in Fig. 4) or assumed (C) geometry were carried out by several post HF methods, and the refinements of the total energy for the LS state were conducted by the spin projection procedures.[8-10] The energy gaps between the LS and HS states at the key

TABLE 3 Energy differences[a](cm^{-1}) between the HS and LS states of bismethylene methane[b] (1a) by several computational methods[c]

Method	[A]	[B]	[C]	[D]
UHF	1132	962	761	1018
APUHF	1704	1447	1115	1504
PUHF(l=1)[d]	144810	154746	19509	154874
PUHF(l=2)	4690	4421	4620	4494
PUHF(l=3)	1207	970	579	1042
UNO-CAS[4,4][e]	1045	832	417	846
UMP2	1097	890	559	1004
APUMP2	1650	1339	839	1453
PUMP2(l=1)[d]	144469	154375	19017	154554
PUMP2(l=2)	4352	4051	4082	4175
PUMP2(l=3)	861	594	105	717
MRSDCI[f]	1355	1075	719	1165
UMP4	996	796	451	892
APUMP4	1498	1196	677	1292
PUMP4(l=1)[d]	144130	154047	189793	154204
PUMP4(l=2)	4015	3725	3703	3826
PUMP4(l=3)	519	263	-279	363
MRSDCI[g]	1485	1188	764	1282
UCCD	965	780	465	873
APUCCD	1452	1172	699	1266
UHF QCISD	954	756	412	853
UHF QCISD(T)	946	749	392	844
APUHF QCISD(T)	1424	1126	589	1221

a) [A] : at the optimized geometry of the highest spin (HS) state
[B] : at the optimized geometry of the lowest spin (LS) state
[C] : at the assumed geometry
[D] : adiabatic energy difference between the LS and HS states
b) the geometries (A-C) are given in Fig.3, c) 6-31G* basis set is used.
d) level of spin projection (see appendix), e) [m,n] : m-active orbitals n-active electrons, f) multi reference CI, g) Davidson correction

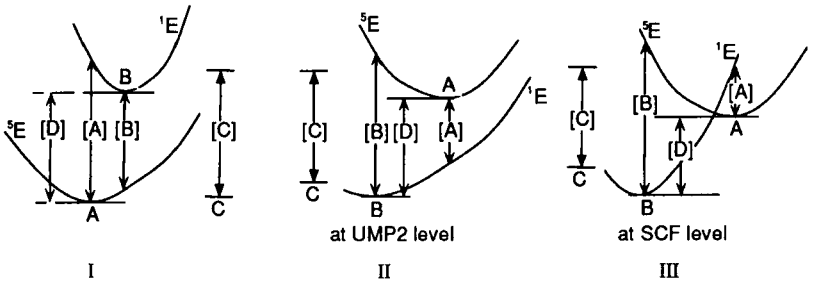

FIGURE 4 The energy gaps between the quintet and singlet states [X] at the geometries X= (A,B,C) in fig. 3 and the adiabatic gap [D] between the optimized geometries of each spin states

points of the potential energy surfaces were determined from these total energies as illustrated in I of Fig. 4. Table 3 summarizes the calculated results. From Table 3, the following conclusions can be drawn:

(1) The four different LS-HS energy differences [A]-[D] are positive by all the computational methods except for the triply projected UMP4 calculation: PUMP4 (l=3) at the assumed geometry. Then bismethylene methane with the the C_{2v} geometry is a HS (S=2) ground-state molecule.

(2) The energy differences obtained by the UHF CCD (UCCD), QCISD, QCISD(T) and MP4 methods at each geometry are quite similar.

(3) The energy differences by UMPn, QCISD and QCISD(T) increase by 40-50 % after the approximate spin projection.

(4) The energy differences by the above UHF based post HF methods are close to those of the spin-symmetry adapted post HF calculations: namely CAS-type multiconfiguration self-consistent field (MCSCF) and multireference (MR) configuration interaction (CI) calculations.

(5) The energy difference after Schlegel's spin projection [9]: PUMPn(l=1) becomes abnormally large, indicating that the single anihilation procedure breaks down in this system, and Handy's double projection scheme[10] :PUMPn (l=2) also leads to the overestimation of the energy gaps, as compared with those of QCISD and MRCI, because of the multiple bond splittings. The triple projection: PUMPn (l=3) rather underestimates the energy gaps because of the over stabilization of the LS state.

(6) The UHF and APUHF methods provide reasonable energy gaps as compared with those of advanced post HF methods such as APUHF QCISD(T).

Since the UHF-type wavefunctions mainly involve the spin polarization (SP) type exchange correlation, the SP mechanism can be applicable to qualitative explanation of the HS ground state of bismethylene methane system; namely $\ddot{C}H$ (↑)-CH_2(↓)-$\ddot{C}H$(↑) in our SP rule.[2] This indicates that the methylele group (-CH_2-) is one of the useful through-bond

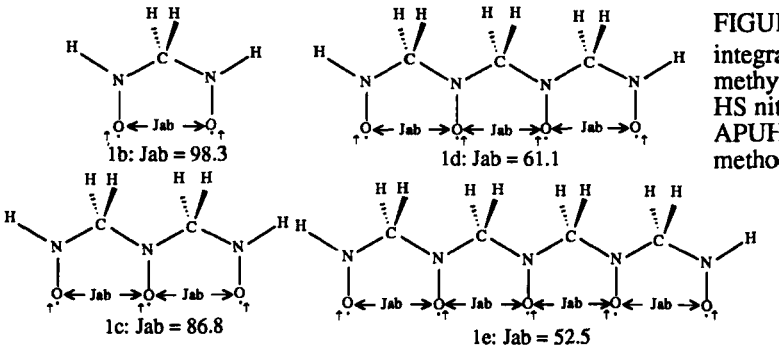

FIGURE 5 Exchange integrals(cm^{-1}) for methylene bridged HS nitroxides by the APUHF STO-3G method

bridges in order to design HS molecules. For confirmation of the SP mechanism, the APUHF calculations were carried out for other systems: namely nitroxide clusters **1b** - **1e** connected by the methylene bridge. The effective exchange integrals Jab between the nearest nitroxide groups were obtained the APUHF STO-3G method (by eq. 4 in the appendix). Figure 5 shows the calculated results. The calculated Jab-values are positive in sign, showing that these nitroxide clusters **1b** - **1e** are HS ground-state molecules in accord with our qualitative predictions based on the SP mechanism.

Spin Delocalization Mechanism

The spin delocalization (SD) mechanism[2] for organic polyradicals with hetero atoms is quite similar to the super exchange (SE) mechanism [11] for transition metal complexes, for example:

$$(\uparrow)\,R\text{———}\underset{\mathbf{2}}{O}\text{———}R\,(\downarrow) \qquad\qquad (\uparrow)\,MLn\text{——}O\text{——}LnM\,(\downarrow)$$

The SE interactions in the binuclear transition metal complexes (M=Cr, Mn, Fe; Ln=ligands) have already been examined by the APUMP methods.[11] It was found that the calculated results are compatible with the experimental results available.

As a continuation of the previous work[11], the post HF calculations were carried out for a simple organic system : $H\ddot{C}\text{-}O\text{-}\ddot{C}H$ (**2a**;X=Y=-$\ddot{C}$H in the case of **2** in Fig. 1) with an appropriate assumed geometry. Table 4 summarizes the total energies of the LS and HS states, and the resulting HS-LS energy differences. The energy differences obtained by all the computational methods employed are negative (antiferromagnetic), indicating the LS (S=0) ground state of **2a**. The magnitudes of the energy differences by APUMP4(2), UHF QCISD, QCISD(T) and PUMP4 (l=3) with the 6-31G* basis set are in the same order, whereas the values by UHF and APUHF correspond to 1/2 -1/4 of the post HF values. The magnitude of the energy gap by the single anihilation procedure[9] is very large because of the overestimation of the stability of the LS state.

The antiferromagnetic exchange interaction between triplet methylene via an oxygen atom is explained by the SD mechanism, which arises from the configuration mixing of the LS ionic structures formed by the intramolecular charge transfer (CT) (namely spin delocalization) as illustrated in Figs. 6A and 6B. The contributions of these structures become large after the correlation correction, giving rise to the increase of the LS-HS gap for **2a**. The SD type through-bond exchange coupling between radical groups is generally expected for other hetero-atom bridges such as S, NH, etc. In order to confirm the SD mechanism, the APUHF STO-3G calculations were carried out for the nitroxide oligomers **3a** -**3d** linked with the NH group as shown in Fig. 7. From Fig. 7, the effective exchange integrals obtained are indeed negative (antiferromagnetic), showing that the SD (or SE)

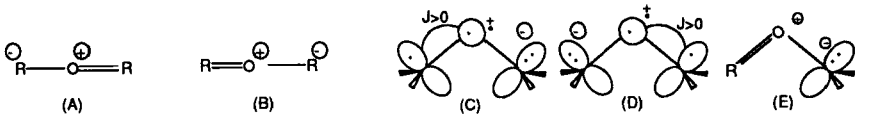

FIGURE 6 Zwittterionic structures (A,B,E) for planar and half planar conformation and the ion radical structures (C,D) for nonplanar bismethylene ether (**2**).

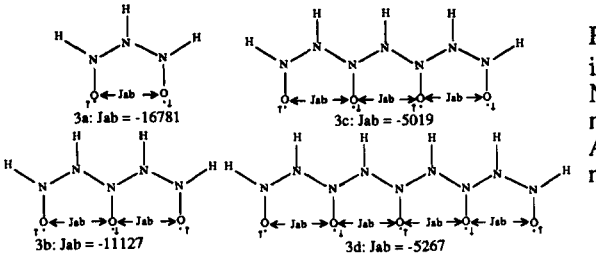

FIGURE 7 Exchange integrals (cm^{-1}) for NH bridged LS nitroxides by the APUHF STO-3G method

mechanism is operative for the nitroxide oligomers **3a** - **3d** examined.

Relations to Experimental Results

Ito, Takui, and Teki, and their collaborators[12] have extensively investigated the through-bond exchange couplings of triplet aromatic carbenes via the methylene or oxygen bridge. They have demonstrated that some of polycarbenes constructed by the through-bond coupling via the methylene bridge have HS ground states, whereas corresponding species with the oxygen bridge are usually the LS molecules.[12]

Here, the APUHF STO-3G calculations were carried out for bisphenylcarbene compounds with the CH_2- and O-bridges; **1f** and **2b**. The effective exchange integrals Jab were calculated by eq. 4 (see appendix) by changing the disrotational angle (Θ) as illustrated in Figs. 8A and 8B. The Jab-values are calculated to be positive (feromagnetic) for **1f** in the whole region of the rotational angle (Θ). On the other hand, the calculated Jab-values are negative for the almost coplanar conformation of **2b** ($\Theta < 45°$), whereas they become positive in its nonplanar conformation ($\Theta > 45°$).

The spin crossover from the singlet to quintet state occurs with the increase of the rotational angle (Θ) of **2b**. The 90° -type superexchange (SE) mechanism or the orthogonal orbital interaction [11] is expected for the heavily torsional conformations (C, D in Fig. 6), leading to the ferromagnetic exchange interaction.

On the other hand, the antiferromagnetic exchange interactions are still predominant in the case of the unsymmetrically distorted structure (E in fig. 6) as in the case of **1a**. The general tendencies revealed by these model calculations are in accord with experimental conclusions by Ito, Takui and Teki.[12] The SP mechanism is also applicable to the bismethylene doubly bridged system, which is extensively investigated by Dougherty and his collaborators.[13]

TABLE 4 Energy differences (cm^{-1}) between the HS and LS states calculated for CHOCH[a] by several computational methods[b]

Method	$^{LS}E_{total}$	$^{HS}E_{total}$	$\Delta E_{total}(cm^{-1})$[c](Jab)[d]
UHF	-151.517680	-151.515139	-558
APUHF	-151.518908	-151.515139	-827(-138)
PUHF(l=1)[e]	-152.177262	-151.518902	-144459(-24077)
PUHF(l=2)	-151.511537	-151.518879	-1611(-269)
PUHF(l=3)	-151.524828	-151.518879	-1305(-218)
UMP2	-151.856780	-151.848017	-1923
APUMP2	-151.860968	-151.848017	-2842(-474)
PUMP2(l=1)[e]	-152.516299	-151.850458	-146100(-24350)
PUMP2(l=2)	-151.850629	-151.850439	-42(-70)
PUMP2(l=3)	-151.863916	-151.850439	-2957(-493)
UMP4	-151.894509	-151.884212	-2259
APUMP4	-151.899431	-151.884212	-3339(-557)
PUMP4(l=1)[e]	-151.553900	-151.885705	-146617(-24436)
PUMP4(l=2)	-151.888372	-151.885688	-589(-98)
PUMP4(l=3)	-151.901610	-151.885688	-3494(-582)
UCCD	-151.880342	-151.872424	-1737
UHF QCISD	-151.891616	-151.878593	-2858
UHF QCISD(T)	-151.900396	-151.886970	-2946

a)R(CO)=1.34 Å; <COC=120°; <HCO=136° b) 6-31G* basis set is used.
c) see eq.1, d) effective exchange integral for the isotropic Heisenberg model
e) level of spin projection. (see appendix)

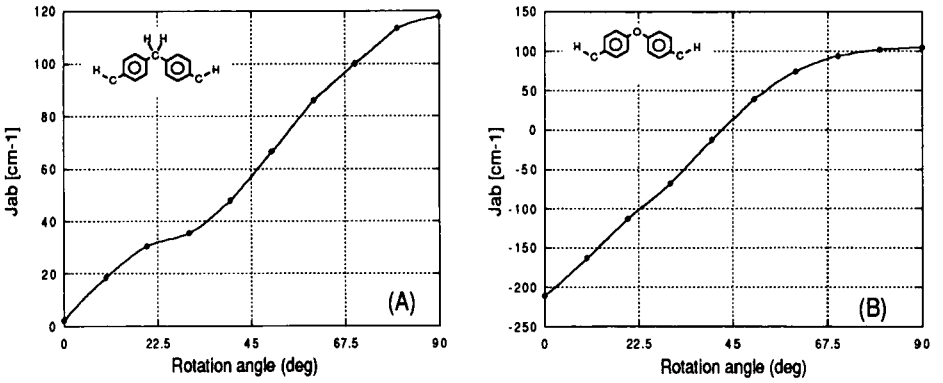

FIGURE 8 Variations of Jab-values with the internal rotation (Θ) of phenyl groups in the case of phenyl carbene dimers linked with methylene (A) and oxygen (B) bridges.

THROUGH-BOND COUPLINGS VIA Π-NETWORK

Post Hartree-Fock Calculations

The through-bond coupling of radical groups via π-networks is of particular importance in relation to molecular design of high-spin polymers (oligomers) by the magnetic modification of conducting polymers with the introduction of radical groups.[2] The APUHF calculations have already been carried out for polycarbenes formed by the through-bond couplings via π-networks.[2] The computational results have shown that the dynamic SP rule in Table 2 is applicable to molecular design of the HS polycarbenes and related species.

(A) through-bond coupling via vinyl group

First, the post HF calculations were performed for C_4H_4 (**4**). Figure 9 illustrates the fully optimized geometries of the HS(A) and LS(B) states of **4** by the UMP2 energy gradient technique, together with the assumed structure (C). From Fig. 9, the optimized structure in the HS (s=2) state is regarded as bismethylene ethylene (HC̈-CH=CH-C̈H), whereas it is rather close to the dehydrobutadiene (HĊ=CH-CH=ĊH) for the LS state.

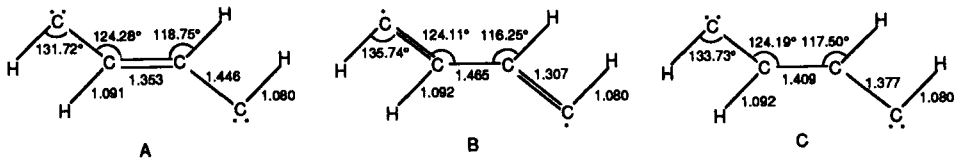

FIGURE 9 Optimized geometries of C_4H_4 in the quintet (A) and singlet (B) states by the UMP2 6-31G* method and the assumed structure (C).

Table 5 summarizes the vertical energy gaps [A]-[D] at the optimized and assumed geometries, and the adiabatic gap in the last column. From Table 5, the following conclusions are drawn:

(1) The four different energy differences are negative by all the post HF calculations. This indicates the LS ground state for **4**. The characteristic features of the potential curves are schematically given by II of Fig. 4.

(2) The vertical energy difference at the optimized HS structure is calculated to be positive by the UHF, APUHF and PUHF levels, although the adiabatic energy difference is negative even in these SCF level of calculations. The profiles of the potential curves are therefore given by III of Fig. 4.

(3) The energy gaps by the UHF based post HF methods except for the single anihilation UMPn (PUMPn(l=1) are in the same order with those of the spin-symmetry adapted methods such as UNO-CAS and MR CI.

The above results indicate that the full geometry optimization is desirable before performing the energy gap calculations. The LS ground states of **4** is consistent with the dynamic SP rule for polyradicals[2]; namely CH(↑)=CH(↓)-CH(↑)=CH(↓).

(B) through-bond coupling via phenyl group

Previously the through-bond couplings of triplet methylenes via the phenyl and other aromatic groups have been investigated by the APUHF STO-3G method.[2] The computational results indicated that the dynamic SP rule is applicable to qualitative predictions of their ground spin states. Here the post HF calculations of m-methylene phenyl methylene **5a** (**5** with X=Y=-CH in Fig. 1) are carried out in order to elucidate the reliability of the SCF level of calculations.[2] The full geometry optimizations of the LS and HS states of **5a** with the C_{2v}, C_2 and C_s symmetries were carried out by the use of UHF 4-31G (STO-3G) energy gradient technique. These computations indicated that the C_{2v} structure is the most stable among them. Figure 10 illustrates the optimized C_{2v} structures of the HS and LS states by the 4-31G(STO-3G in parentheses) method. The vertical

TABLE 5 Energy difference[a)] (cm^{-1}) between the HS and LS states calculated for C_4H_4[b)] by several computational methods[c)]

Method	[A]	[B]	[C]	[D]
UHF	2578	-25408	-17196	-12676
APUHF	3153	-34487	-24853	-21756
PUHF(l=1)[d)]	934	-67678	-157178	-55004
PUHF(l=2)	2743	-26150	-14994	-13471
PUHF(l=3)	2628	-30713	-23533	-18035
CAS[4,4]	-9307	-25912	-16641	-13778
UMP2	-8736	-23592	-14397	-13897
APUMP2	-10670	-27894	-20232	-21593
PUMP2(l=1)[d)]	-10654	-65880	-154384	-56211
PUMP2(l=2)	-8852	-24642	-12492	-14967
PUMP2(l=3)	-8966	-29132	-20943	-19485
MRSDCI[e)]	-12243	-31290	-19478	-47883
UMP4	-10260	-24311	-15172	-14573
APUMP4	-12531	-32243	-21321	-22506
PUMP4(l=1)[d)]	-12344	-66342	-154910	-56613
PUMP4(l=2)	-10573	-25568	-13478	-15834
PUMP4(l=3)	-10686	-29942	-21788	-20208
MRSDCI[f)]	-13142	-28021	-20090	-18500
UCCD	-8679	-24545	-15270	-14189
APUCC	-10600	-32553	-21459	-22197
UHF QCISD	-10745	-27257	-18415	-17237
UHF QCISD(T)	-13066	-27242	-18704	-17745
APUHF QCISD(T)	-15999	-36130	-26284	-26634

a) [A] at the optimized geometry for the quintet state by the UMP2 method
[B] at the optimized geometry for the singlet state by the UMP2 method
[C] at the assumed geometry
[D] the adiabatic energy difference between the LS and HS states
b) see Fig.9,c) 6-31G* basis set is used,d) level of spin projection (see appendix)
e) Multireference single double CI, f) after Davidson correction

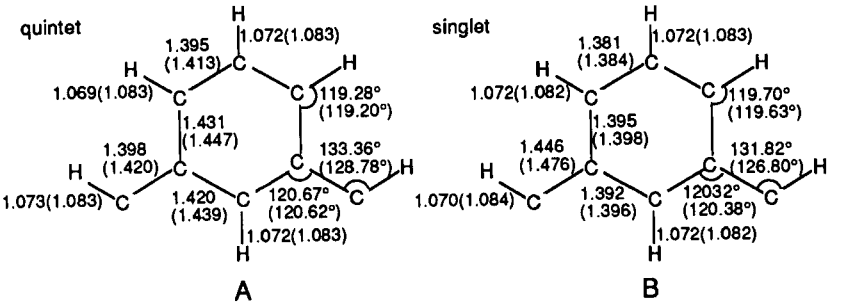

FIGURE 10 Optimized geometries of the quintet (A) and singlet (B) of C_8H_6 with the C_{2v} structure by the UHF 4-31G (STO-3G values in parentheses) method.

energy gaps at the optimized HS geometry by the UHF 4-31G method were calculated by the post HF methods by the use of the STO-3G basis set. Table 6 summarizes the calculated results. From Table 6, the following conclusions are drawn:

(1) The UHF, APUHF and PUHF(l>2) provide quite large positive energy gaps, showing the HS ground state of **5a**.

(2) The UMPn (n>2) methods give the negative energy difference, showing the LS ground state. The approximately spin projected version (APUMPn) cannot change this tendency because of its simple projection scheme (see eq. 4 in the appendix).

(3) The PUMPn(n>2) method by the use of Lowdin's projection scheme[14], however, predicts the positive difference; namely the HS ground state.

4) The UHF coupled-cluster (CC) method by the use of the double (D) excitation operator (UCCD) predicts the LS ground state. The situation is the same for its approximately spin projected version (APUCC).

(5) The UHF QCISD and QCISD(T) methods, together with their approximately projected version (APUHF QCISD and QCISD(T)), predict the HS ground state.

The above conclusion (4) implies that the LS radical state is much more stabilized than the HS radical state by the configuration mixing of doubly excited configurations, which are chemically described by zwitterionic (ZW) structures (namely spin delocalized forms) as illustrated in Fig. 11. However, the conclusion (5) indicates that the HS radical state is more stabilized than the LS radical state by the inclusions of single (S) and triple (T) excitation operators in the QCI scheme, which are responsible for the spin polarization (SP) effect. The net effect of both the contributions gives rise to the decrease of the HS-LS gap, but the HS state remains in the ground state in the case of **5a** because the SP effect overweighs the SD effect as illustrated in A of Fig. 12. On the other hand, the HS-LS inversion may occur if the contribution of ZW configurations becomes predominantly important as illustrated in B of Fig. 12.

Comparison with Experiments

The magnitudes of Jab-values for **5a** are found to be sensitive to the levels of computational methods and basis set used, together with the geometries employed. Fortunately, the APUHF STO-3G and QCISD(T) methods predict the same HS ground state, although the former overestimates the magnitude of Jab since it includes no dynamical correlation correction: a scaling factor f should be introduced in order to estimate reasonable Jab-values by the latter method by the use of those of the former as follows:

$$f = \Delta E_{total}\,(\text{APUHF QCISD(T)})/\Delta E_{total}\,(\text{APUHF}) = 1/14 \qquad (2)$$

TABLE 6 Energy difference (cm^{-1}) between the HS and LS states calculated for C_8H_6[a] by several computational methods[b]

Method	$^{LS}E_{total}$	$^{HS}E_{total}$	$\Delta E_{total}(cm^{-1})$(Jab)[c]
UHF	-302.499672	-302.576678	16903
APUHF	-302.467247	-302.576678	24020(4003)
PUHF(l=1)[c]	-302.083812	-302.617664	117182(19530)
PUHF(l=2)	-302.480878	-302.608155	27938(4656)
PUHF(l=3)	-302.507120	-302.608984	22360(3727)
PUHF(l=4)	-302.505956	-302.608950	22608(3768)
CAS[4,4]	-302.484738	-302.489289	999
UMP2	-302.890695	-302.875113	-3420
APUMP2	-302.897514	-302.875113	-4917(-820)
PUMP2(l=1)[d]	-302.474773	-302.911994	95971(15995)
PUMP2(l=2)	-302.871818	-302.903128	6873(1146)
PUMP2(l=3)	-302.898138	-302.903777	1238(206)
PUMP2(l=4)	-302.896977	-302.903747	1486(248)
UMP4	-302.975521	-302.963570	-2623
APUMP4	-302.980751	-302.963570	-3771(-629)
PUMP4(l=1)[d]	-302.559536	-302.994778	95537(15923)
PUMP4(l=2)	-302.956572	-302.986757	6626(1104)
PUMP4(l=3)	-302.982958	-302.987168	924(154)
PUMP4(l=4)	-302.981799	-302.987142	1173(196)
UCCD	-302.979973	-302.966089	-3048
APUCCD	-302.986049	-302.966089	-4381(-730)
UCCDST4	-302.994880	-302.985091	-2149
AUCCDST4	-302.999164	-302.985091	-3089(-515)
UHF QCISD	-302.985204	-302.995434	2246
APUHF QCISD	-302.980727	-302.995434	3228(538)
UHF QCISD(T)	-302.998533	-303.003875	1173
APUHF QCISD(T)	-302.996195	-303.003875	1686(281)

a)at the quintet optimized geometry(4-31G) (see Fig. 10),b) STO-3G basis set is used,c) effective exchange integral for the isotropic Heisenberg model
d) level of spin projection.

The scaling significantly improves the magnitudes of Jab-values obtained for various phenyl polycarbenes by the previous APUHF STO-3G calculations.[2]

Figure 13 shows the molecular structures of meta-phenylene bridged methylene oligomers **5b-5e** with the planar assumed geometries. The calculated Jab-values are largely positive by the APUHF STO-3G method, indicating the HS ground state for **5b-5e** in accord with experiments [15,16] The magnitude of Jab is reduced by the use of the 4-31G basis set, but it is much larger than the corresponding INDO value. However, the scaled Jab-values in parentheses by eq. 2 are reasonable as compared with the experiments.[15,16] The SP rule is applicable to qualitative explanation of the HS ground states of **5b-5e**.

The APUHF STO-3G calculations were performed with changing the rotational angle (Θ) of bismethylene group in the case of metha (**5a**) and para (**6**) phenylene bis(methylene) with the assumed C-C bond lengths. Figure 14 shows the variation of Jab with Θ. From Fig. 14, the signs of Jab remain positive and negative for **5a** and **6**, respectively, throughout the internal rotation, although the magnitudes of Jab are reduced significantly in the distorted conformation in both the cases. The signs of Jab-values for **5a** and **6** are in agreement with the SP rule.[2]

The variations of Jab with the diheral angle (Θ) of (3,4')- and (4,4')-biphenyl bismethylenes (**7**, **8**) were also examined by the APUHF STO-3G method. The results are summarized in Table 7. The signs of Jab are not changed with the nonplanarity of **7** and **8** in accord with the SP rule, although the magnitude of Jab decreases with the increase of Θ. The scaled Jab-values for **5-8** are consistent with experimetal results by Ito-Takui and their collaborators[15] and Iwamura and his collaborators.[16]

There are several interesting examples which indicate the violation of the SP rule even for metha-phenylene bridged systems. According to Iwamura[16] and Rassat[17], dinitroxide (**9a**: X=-NO(t-Bu), Y=H, Z= t-Bu in Fig. 11) has the HS (triplet) ground state, whereas dinitroxides (**9b**: X=-NO(t-Bu), Y=-OCH_3, Z= H in Fig. 11, and its planar analog **9c**) have the LS (singlet) ground state. Their experiments imply that the contribution of zwitterionic configurations (B, C in Fig. 11) is not negligible in the case of dinitroxides with electron donating groups such as methoxy group, and the HS-LS inversion is induced by the configuration interaction (CI) as illustrated in B of Fig. 12. Judging from the numerical results in Tables 3-6, extensive CI computations such as MRSDCI, QCISD(T), etc. are necessary for theoretical determinations of the sign and magnitude of Jab-values for **9a-9c**. The basis sets should be also flexible enough for CI calculations of such hetero atom systems. Therefore reliable computations for **9a-9c** are interesting future problems.

POSSIBILITIES OF FERROMAGNETIC CONDUCTORS (METALS)

The introductions of hole or electron into magnetic systems have received current interest in relation to possibilities of organic magnetic conductors (metals), spin-mediated

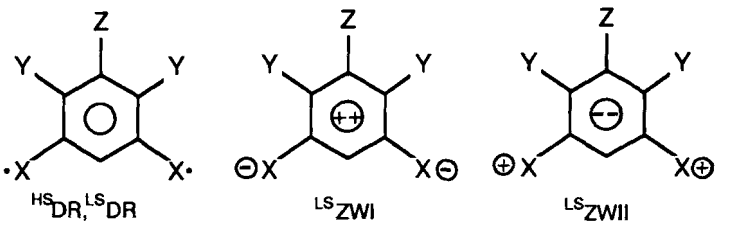

FIGURE 11 Diradical (DR) and zwitterionic (ZW) configurations for m-phenylene bridged system. Y and Z denote polar substituents introduced.

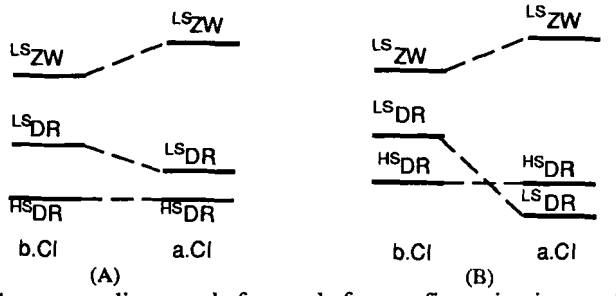

FIGURE 12 The energy diagrams before and after configuration interaction (CI). The HS-LS relative stability is the same even after CI in the case A, whereas it is reversed in B.

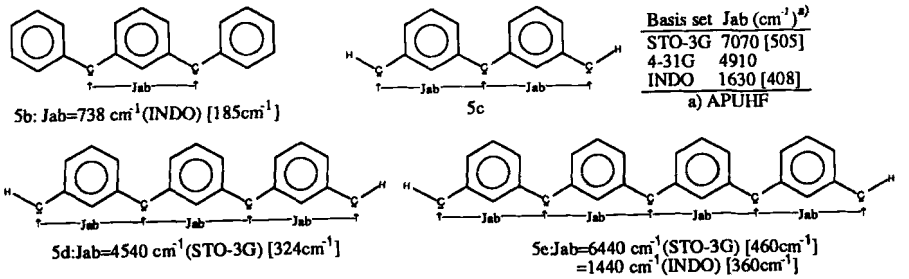

FIGURE 13 Through-bond exchange couplings for high-spin polycarbenes (the scaled Jab-values are in parentheses).

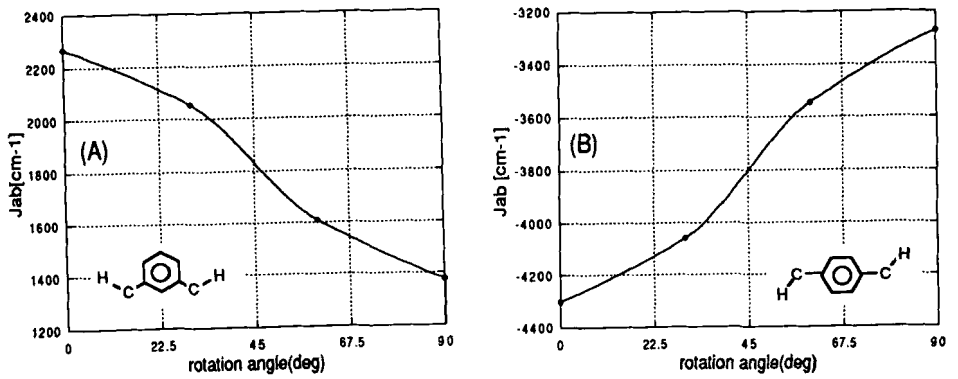

FIGURE 14 Variations of Jab-values with disrotatory distortion (Θ) of methylene groups of metha (A) and para (B) phenyl bismethylene with assumed geometries.

Table 7 Effecive exchange integrals Jab(cm^{-1})[scaled values]for biphenyl-bismethylene

	Position			Position	
θ(deg)	(3,4')	(4,4')	θ(deg)	(3,4')	(4,4')
0°	1154[82]	-1319[-94]	60°	460[33]	-496[-35]
30°	919[66]	-1033[-74]	90°	221[16]	-229[-16]

superconductors, and so on.[4] Previously APUHF calculations were carried out in order to elucidate such possibilities with the introduction of hole or electron: namely one-electron oxidation or reduction.[2,4] Here, the post HF calculations[6] were carried out for the confirmation of previous results.[2,4]

Post HF Calculations

The post HF 4-31G calculations were carried out for the mono cation and anion radical states of C_4H_4 (**4**) with the three assumed geometries given in Fig. 15. Table 8 summarizes the energy differences between the LS(S=1/2) and HS(S=3/2) states. From Table 8, the mono cation and anion of **4** have the HS and LS ground states, respectively. The sign of Jab is reversed upon the hole introduction into the π-electron system. While the captured electron enters into the σ-orbital in the case of mono anion of **4**, forming the lone pair. The CASSCF [6,n] calculations indicated that the situations are not changed with the internal rotation of the terminal CH groups of both the cation (n=5) and anion (n=7) states of **4**. Thus the CASSCF calculations for **4** support the previous conclusion obtained for cation radicals of polycarbenes with vinyl coupling unit by the APUHF STO-3G computations, although the energy differences between HS and LS should be improved by the scaling (eq. 2).

Comparison with Experiments

Shida, Ito and Takui's group[18] have initiated the experiments, showing that the one-electron reduction of m-phenylene bis(phenylmethylene) **7b** generates the corresponding HS radical ions: the qurtet ground state (S=2-1/2=3/2). The APUHF INDO calculations were already carried out for the mono cation and anion states of m-phenylene bridged carbene systems.[5b-

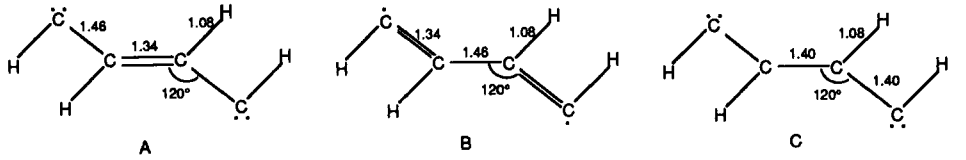

A B C

FIGURE 15 Bismethylene ethylene (A), dehydrogenated butadiene (B) and uniform (C) structures assumed for hole or electron-doped C_4H_4.

Table 8 Energy differences between the HS and LS states calculated for electron or hole doped C_4H_4[a] by several computational methods[b]

Method	[A] Cation	[A] Anion	[B] Cation	[B] Anion	[C] Cation	[C] Anion
UHF	3777	-1503	3329	-2832	3576	-1979
APUHF	5149	-1844	4629	-3052	4919	-2276
UMP2	2856	-1658	2279	-3863	2443	-2565
APUMP2	3697	-2008	3315	-4141	3520	-2917
UMP4	2304	-1944	2044	-4178	2180	-2877
APUMP4	3294	-2354	3291	-4478	3142	-3272
UNO-CAS[c]	3228	-3002	530	-4917	652	-3838

a) geometries in Fig.14, b) 4-31G basis set
c) Active space; Cation [6-orbitals 5-electrons]; Anion [6-orbitals 7-electrons]

5d.[19] Table 9 summarizes the calculated results. Both the one-electron oxidation and reduction of the HS neutral carbenes with the (2S+1) spin multiplicity provide, respectively, the corresponding HS cation or anion radicals with the 2S spin multiplicity. As illustrated in Fig. 16, the (2S+2) spin state arising from the ionization of β-electron or β-electron capture was not the ground spin state in the m-phenylene bridged systems examined here. The hole or electron dopings of **5b**-**5d** do not give rise to the LS-HS inversion, namely the reversion of the sign of Jab. The situation is the same in the case of the (2,3')-substituted pyrrole dimer examined previously.[2] The SP mechanism is predominantly operative for the ions of these species, in a sharp contrast to some polycarbene systems[2] linked with vinyl (**4**), biphenyl (**7**,**8**) and naphtalene groups in fig.1, for which the SP mechanism is relatively weak even in the neutral state.[2]

In order to confirm the importance of the SP effect in polycarbenes, the APUHF compu-tations were also performed for the cation and anion radicals of metha-phenylene bridged trimethyl radical (**10a**)(namely triplet methylene is replaced by doublet methyl radical in **5c**). The total energies are shown in Table 9. From Table 9, the LS (singlet) state becomes a little more stable than the HS (triplet) state in both the cases. This indicates the important contributions of the ionic configurations in the singlet state; CH2 (↑) -Ph-CH(+)-Ph-CH2(↓) and CH2 (↑) -Ph-CH(-)-Ph-CH2(↓). If so, the substitution of H by Ph in **10a** may provide the HS (triplet) ion radicals since contributions of such ionic configurations become weak. Thus the ground spin states for ion radicals are determined by subtle balance between the SP and SD effects. The comparison of calculated results for **10a** and **5c** clearly indicates that the σ-π exchange interaction enhances the SP effect of π–electron networks in polycarbene systems. A similar situation is also noticed in the case of nitroxides as discussed

Table 9 The total energies of the hole and electron-doped phenylcarbenes and related species[a)]

System	2S+1	cation	anion
[Ph-C̈-Ph]	2	-95.77384	-96.03338
	4	-95.74287	-95.93788
[Ph-C̈-Ph-C̈-Ph] (**5b**)	2	-146.15961	-146.48222
	4	-146.24789	-146.52582
	6	-146.24180	-146.43049
[HC̈-Ph-C̈-Ph-C̈H] (**5c**)	2	-108.74775	-109.04077
	4	*	-109.05003
	6	-108.81477	-109.08373
	8	-108.80450	-108.99198
[HC̈-Ph-C̈-Ph-C̈-Ph-C̈H] (**5d**)	2	-159.13559	-159.48557
	4	-159.23844	-159.51394
	6	-159.26537	-159.54335
	8	-159.31220	-159.57282
	10	-159.30215	-159.47925
[H_2Ċ-Ph-ĊH-Ph-ĊH_2](**10a**)	1	-111.74546	-112.03752
	3	-111.74370	-112.03600
	5	-111.73024	-111.91370
[C_4H_5-Ph-C_4H_4-Ph-C_4H_5][c)] (**11a**)	1	-909.92346	
	3	-909.94265	

a) the most stable state is underlined, b) the INDO UHF method is used, * not converged, c) STO-3G basis set used for the dication of this polyene.

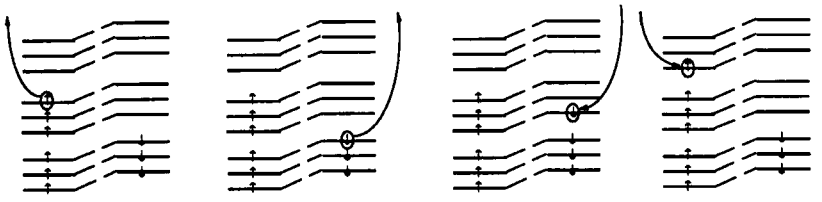

FIGURE 16 Possible spin states of the hole (A,B) and electron (C,D) doped states of the HS molecules with the (2S+1) spin multiplicity.

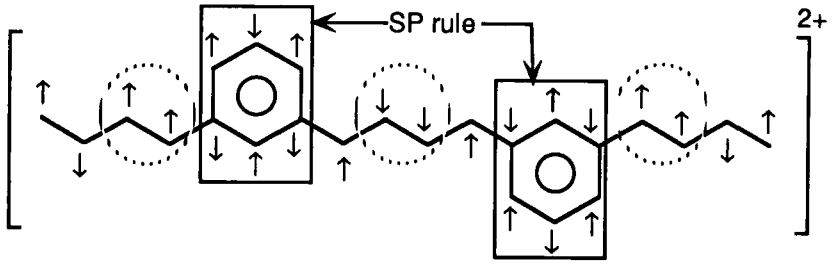

FIGURE 17 Spin density popolations of the dication of 11a by the APUHF STO-3G method. The parallel induced-spin alignment s are recognized in the circles, showing the polaronic behavior. However, the spacer parts exhibit the SP-type spin density populations.

previously.[20]

The previous APUHF calculations[2] have indicated that the SP effect for m-phenylene bridge (**5**) is of particular importance even when the ion radicals such as cation radicals of anino groups are used as spin sources. As an example, let us consider a polyene (**11a**), which is constructed by the substitution of methylene in **5a** or methyl in **10a** by butadiene group. The APUHF STO-3G calculations were carried out for the dications of **11a**. The results are given in Table 9. Table 9 shows that **11a** has the HS (triplet) ground state, and the scaled Jab-value is about 300 cm^{-1}. Figure 17 illustrates the pattern of spin density populations in the HS state of **11a**. The parallel induced spins appear within the butadiene skeletons, supporting the polaronic cation radical state suggested by Fukutome[21] and Dougherty[22]. Interestingly, the spacer part or coupling unit (phenyl ring) exhibit, however, the normal SP pattern recognized for many other m-phenylene bridged systems. Therefore, the SP rule for ion radical species[2] is applicable to **11a**. This in turn indicates that polycationic states of polaronic ferromagnetic polymers might not have the HS ground states when the singlet bipolarons are formed within the chains even when the m-phenylene bridge is utilized.

CONCLUSIONS

The present post Hartree-Fock (HF) calculations have clearly demonstated that the previous spin alignment rules[2] summarized in Table 2 and Fig. 2 work well for qualtitative predictions and explanations of the ground spin states of polycarbene systems, related polyradical systems and also ion radical species. However, the numerical results given in Table 3-6 shows that the very accurate computational methods such as MRSDCI and QCISD(T) are necessary for quantitative calculations of the energy gaps between the highest and lowest spin states, namely the effective exchange integrals in the Heisenberg model.

ACKNOWLEDGEMENTS

The author (K.Y.) thanks Professors H. Iwamura, K. Itoh, M. Kinoshita and T. Takui for their stimulating discussions and suggestions. This work was carried out by the aid of the Grant-in-Aid for Scientific Research on Priority Area" Molecular Magnetism" (Area No. 228/04242104) from the Ministry of Education, Science and Culture.

APPENDICES

Here the notations of the post-Hartree-Fock computational methods[6] employed are given as follows: CI: configuration interaction, MR: multireference, MPn: n-th order Møller-Plesset perturbation; CCD: Coupled Cluster involving double (D) excitation operator, QCISD(T) : quadratic configuration interactions (CI) involving single (S) , double (D) and triple (T) excitation operators. Then the correlation correction methods for the unrestricted

Hratree-Fock (UHF) self-consistent-field (SCF) solution are expressed as UMPn: UHF MPn; UCCD: UHF CCD; UHF QCISD, UHF QCISD(T). The spin projections to eleiminate the high-spin components of the LS UMPn wavefunction are referred to as PUMPn(l=1), PUMPn(l=2) and PUMPn(l=m), depending on the single, [9] double[10] and m-tuple projections, respectively. The energy correction by the approximate spin projection of the spin-contaminated post HF wavefunctions for the LS stste is given by

$$\Delta\Delta E = [\ < S^2 >(LS) - S(S+1)\ ]\ Jab \qquad (3)$$

where $< S^2 >(LS)$ and S denote, respectively, the total spin angular momentum calculated by the LS post HF wavefunction and the exact spin quantum number in the LS state. The effective exchange integral Jab is given by the use of eq. 1 in the text as

$$Jab = \Delta E(LS\text{-}HS)/[\ {}^{HS}< S^2 >(X) - {}^{LS}< S^2 >(X)\ ] \qquad (4)$$

The notation of the approximately projected wavefunctions are given as follows: APUHF: AP UHF; APUMPn : AP UHF MPn; APUCCD: AP UHF CCD; APUHF QCISD(T). In this paper, the symmetry-adapted post HF calculations are also performed for comparison with the UHF-based methods. The complete active space (CAS) SCF calculations by the use of the natural orbitals of the UHF solutions as trials are referred to as UNO-CASSCF or UNO-CAS. The multireference (MR) CI correction for the UNO-CAS is referreed to as MRCI.

REFERENCES

1 K. Yamaguchi, Chem. Phys. Lett. 33, 330; 35, 230 (1975).
2. K. Yamaguchi et al., Synthetic Metals 19, 81, 89 (1987).
3 . K. Yamaguchi, Y. Toyoda and T. Fueno, Chem. Phys. Lett. 159, 459 (1989).
4. K. Yamaguchi, Int. J. Qaunt. Chem. 37, 167 (1990).
5. K. Yamaguchi, N. Namimoto and T. Fueno, Mol. Cryst. Liq. Cryst. 176, 151 (1989).
6. The GAUSSIAN and ALCHEMY II program packages were used throughout the present calculations at IMS and IBM RISK 6000 computers.
7. H. Iwamura, Pure Appl. Chem. 59, 1595 (1987).
8. K. Yamaguchi et al, Chem. Phys. Lett. 149, 537 (1988).
9. H. B. Schelegel, J. Chem. Phys. 84, 4530 (1986).
10. P. J. Knowles and N. C. Handy, J. Chem. Phys. 88, 6991 (1988).
11. K. Yamaguchi et al., Chem. Phys. Lett. 143, 371 (1988).
12. K. Ito et al., Mol. Cryst. Liq. Cryst. 176, 49 (1989).
13. D. A. Dougherty et al., Mol. Cryst. Liq. Cryst. 176, 25 (1989).
14. P. O. Lowdin, Phys. Rev. 97, 1509 (1955).
15. T. Takui et al., Mol. Cryst. Lig. Cryst. 176, 67 (1987).
16. H. Iwamura et al., proceeding in this conference.
17. A. Rassat, private communication.
18. M. Matsushita et al., J. Am. Chem. Soc. 114, 7470 (1992).
19. M. Okumura et al., Annual Meeting of Japn Chemical Society p657 (1990).
20 K. Yamaguchi et al., Chem. Lett. 629 (1986).
21 H. Fukutome et al., Chem. Phys. Lett. 133, 34 (1987).
22 D. A. Kaisaki et al., J. Am. Chem. Soc. 113, 2704 (1991).